



HAL
open science

The Molecular Circadian Clock Is a Target of Anti-cancer Translation Inhibitors

Alexandre Berthier, Céline Gheeraert, Manuel Johanns, Manjula Vinod, Bart
Staels, Jérôme Eeckhoute, Philippe Lefebvre

► **To cite this version:**

Alexandre Berthier, Céline Gheeraert, Manuel Johanns, Manjula Vinod, Bart Staels, et al.. The Molecular Circadian Clock Is a Target of Anti-cancer Translation Inhibitors. *Journal of Biological Rhythms*, 2023, 10.1177/07487304231202561 . hal-04264765

HAL Id: hal-04264765

<https://hal.science/hal-04264765>

Submitted on 30 Oct 2023

HAL is a multi-disciplinary open access archive for the deposit and dissemination of scientific research documents, whether they are published or not. The documents may come from teaching and research institutions in France or abroad, or from public or private research centers.

L'archive ouverte pluridisciplinaire **HAL**, est destinée au dépôt et à la diffusion de documents scientifiques de niveau recherche, publiés ou non, émanant des établissements d'enseignement et de recherche français ou étrangers, des laboratoires publics ou privés.

The molecular circadian clock is a target of anti-cancer translation inhibitors

Alexandre Berthier^{1*}, Céline Gheeraert¹, Manuel Johanns¹, Manjula Vinod¹, Bart Staels¹, Jérôme Eeckhoutte¹ and Philippe Lefebvre¹

¹Univ. Lille, Inserm, CHU Lille, Institut Pasteur de Lille, U1011-EGID, F-59000 Lille, France.

*Corresponding author: alexandre.berthier@inserm.fr

Abstract

Circadian-paced biological processes are key to physiology and required for metabolic, immunologic and cardiovascular homeostasis. Core circadian clock components are transcription factors whose half-life is precisely regulated, thereby controlling the intrinsic cellular circadian clock. Genetic disruption of molecular clock components generally leads to marked pathological events phenotypically affecting behavior and multiple aspects of physiology. Using a transcriptional signature similarity approach, we identified anti-cancer protein synthesis inhibitors as potent modulators of the cardiomyocyte molecular clock. Eukaryotic protein translation inhibitors, ranging from translation initiation (rocaglates, 4-EGI1...) to ribosomal elongation inhibitors (homoharringtonine, puromycin ...), were found to potently ablate protein abundance of REV-ERB α , a repressive nuclear receptor and component of the molecular clock. These inhibitory effects were observed both *in vitro* and *in vivo* and could be extended to PER2, another component of the molecular clock. Taken together, our observations suggest that the activity spectrum of protein synthesis inhibitors, whose clinical use is contemplated not only in cancers but also in viral infections, must be extended to circadian rhythm disruption, with potential beneficial or iatrogenic effects upon acute or prolonged administration.

Keywords: Circadian, REV-ERB α , proteostasis, anti-cancer drugs, heart, homoharringtonine.

Introduction

All organisms living on Earth have evolved to temporally modulate physiological regulations allowing metabolic (pre)adaptations to activity and rest periods, which are normally aligned on night and day cycles. Adopting a 24h period, the light-induced pacing of the central nervous system and of connected organs is further controlled by additional Zeitgebers (time givers) such as food intake or social interaction (Fagiani et al., 2022). The importance of these circadian regulations is highlighted by deleterious effects on metabolic homeostasis of an unphased lifestyle, such as shift work or chronic jet lag, which extends organism exposure to artificial light, induces sleep alteration and irregular food intake (Sulli et al., 2018). Whether they are causative or not of diseases in humans is unclear, but misalignments and/or blunting of the internal clock are associated to a large panel of pathologies ranging from cardio-metabolic, immuno-inflammatory diseases and cancer to psychiatric disorders (Baron and Reid, 2014; Jacob et al., 2020; Mukherji et al., 2020; Wang et al., 2022). As a consequence, lifestyle adaptations to minimize or correct these ailments by resetting/rephasing this internal clock is warranted. Targeting the clock is also an entry point for the development of novel, more efficient and less toxic therapeutic strategies (Sulli et al., 2018; Tamai et al., 2018; Ye et al., 2018).

At the cellular level, circadian rhythms are established by 2 autoregulatory loops of transcription factors, encoded by so-called core clock genes (CCGs). The first transcriptional loop is composed of the heterodimeric BMAL1 (ARNTL) and CLOCK transcriptional activators and of PER and CRY transcriptional repressors. The secondary loop is made of the nuclear receptors RORs, REV-ERB α and REV-ERB β . These interlocked transcriptional-translational feedback loops (TTFLs) define a cell-autonomous clock machinery whose temporal regularity is conditioned by the precise orchestration of gene transcription and of protein degradation (Kramer et al., 2022). These TTFLs themselves control clock output genes, which are involved in a myriad of biological processes including metabolism, inflammation and house-keeping functions, underlying again the fundamental role of the molecular clock in organismal homeostatic control (de Assis and Oster, 2021).

Considering the major role of the molecular clock, it seems obvious that any drug treatment altering the clock in normally-phased individuals may be iatrogenic. Importantly, dysregulated circadian rhythmicity is associated with poor survival rates in cancer patients and a few chemotherapeutic agents such as paclitaxel have been shown to disrupt endogenous circadian rhythms (Sullivan et al., 2022). We recently discovered that acute administration of the cardiotoxic steroid digoxin, chronically used to treat atrial fibrillation, severely impacts on TTFLs by promoting the proteasomal degradation of the nuclear receptor REV-ERB α (Vinod et al., 2022). REV-ERB α transcriptional repressive activity is detrimental to myocardial resistance to an ischemia-reperfusion insult (Montaigne et al., 2018). Interestingly, digoxin has also been proposed as a potential anti-cancer drug (Elbaz et al., 2012a; Elbaz et al., 2012b; Zhou et al., 2019; Ren et al., 2021), but its impact on the molecular clock has not been assessed in this context. Broadly speaking, we also note that cancer therapies are significantly associated with cardiac and vascular toxicity with multiple etiologies and mechanisms of action (Herrmann, 2020). Given that circadian rhythmicity is paramount to cardiac physiology, this warrants the specific exploration of chemical anti-cancer molecules in cardiomyocytes.

Thus, to identify drugs which could impact cardiomyocyte biology through a dys-synchrony of the molecular clock, we compared perturbations of the gene expression pattern triggered by digoxin

in a reference human cardiomyocyte cell line to the L(andmark)1000 compendium collected from drug-treated cancer cell lines (Subramanian et al., 2017). Here we report that transcriptional pattern similarities could be identified with structural analogues of digoxin, validating our strategy. More unexpectedly, a significant proportion of digoxin-like molecules belonged to the protein synthesis inhibitor class, including homoharringtonine (HHT, omacetaxine mepesuccinate), an alkaloid approved by the Food and Drug Administration for the treatment of chronic myeloid leukemia. A significant number of tested anti-cancer protein synthesis inhibitors also strongly impacted on REV-ERB α protein synthesis and affected cardiomyocyte circadian rhythmicity *in vitro* and *ex vivo*. We propose an original workflow allowing the identification and characterization of molecules able to target the clock machinery by decreasing REV-ERB α protein levels.

Materials and methods

Reagents

Digoxin (Sigma-Aldrich, D6003) was dissolved in 10% ethanol, 40% propylene glycol, 0.08% citric acid, 0.3% sodium phosphate and stored at 4°C. The 20S proteasome sub-unit inhibitor Clasto-Lactacystin β -lactone (Sigma-Aldrich, L7035) as well as all the other drugs listed in the table below were dissolved in DMSO and stored at -20°C. Rabbit Anti-NR1D1 and mouse anti HSP90 α/β monoclonal antibodies were obtained from Cell Signaling Technology (13418) and BioLegends (661802) respectively.

Drugs

Drug name	CAS number	Supplier	Reference
4EGI-1	315706-13-9	TargetMol	T2665
Anisomycin	22862-76-6	Sigma-Aldrich	A9789
Cephaeline	CAS:483-17-0	MedChemExpress	HY-N4118
Clofarabine	123318-82-1	TargetMol	282T0297
CR-1-31-B	1352914-52-3	MedChemExpress	HY-136453
F-1566-0341	881046-06-6	MolPort	MP-0000-0000-5408-6556
Harringtonine	CAS 26833-85-2	Santa Cruz Biotechnology	sc-204771
Homoharringtonine	26833-87-4	Santa Cruz Biotechnology	sc-202652
LDN-193189	1435934-00-1	Focus Biomolecules	10-4764
MCB-613	296792-62-6	Sigma-Aldrich	SML1567
Narciclasine	29477-83-6	MedChemExpress	HY-16563
Obatoclax	803712-79-0	Focus Biomolecules	10-2660
Puromycin	53-79-2	InvivoGen	Ant-pr-1
Rocaglamide A	84573-16-0	MedChemExpress	HY-19356
Salubrial	405060-95-9	TargetMol	T3045
Silvestrol	697235-38-4	MedChemExpress	HY-13251
Verrucarine A	3148-09-2	Sigma-Aldrich	V4877
YM-155	781661-94-7	Focus Biomolecules	10-1473

Animal Experimentation

Mice were handled in accordance to institutional guidelines and approved by the local ethics committee for animal experimentation (Comité d'Éthique en Expérimentation Animale n°075). C57bl/6J mice were purchased from Charles River Laboratories and Per2::luc mice [IMSR_JAX:006852 (Yoo et al. 2004)] were from The Jackson Laboratory and were re-derived into SOPF C57bl/6J mice at Charles River Laboratories. Animals were housed in a 12h/12h light/dark cycle and fed ad libitum with a chow diet (Safe diets, A04) and free access to drinking water. For acute *in vivo* experiment, 11 weeks old wild type males were first acclimated for 2 weeks in the animal facility. On the day of the experiment, HHT 1 mg/kg, a dose chosen according previous studies (Li et al., 2020; Wang et al., 2021) or control vehicle (0.25% DMSO in 9 g/L NaCl solution) were administrated by intra peritoneal injection at ZT5. Animals were then sacrificed at ZT9 by cervical dislocation and hearts were cut in half, flash-frozen in liquid nitrogen and stored at -80°C. For the *ex vivo* atrial explant experiment, 23

week-old Per2::Luc males were used. Briefly, animals were sacrificed by cervical dislocation at ZT 7 (ZT0 is light on), atria were collected, washed in ice-cold 1X PBS and cut in 2 mm³ pieces.

Cell lines

The human ventricular cardiomyocyte cell line AC16 was purchased from Merck-Millipore (SCC109) and maintained in DMEM/F12 Ham medium (Sigma-Aldrich, D6434), supplemented with 2 mM L-glutamine (Thermo Fisher Scientific), 12.5% fetal calf serum (FCS) and 1% penicillin-streptomycin (Thermo Fisher Scientific).

Human primary ventricular cardiomyocytes (HPC) were isolated from a male donor after a cardiac transplantation. These cells were obtained from PromoCell (C-12811) and maintained in Myocyte Growth Medium (C-22070, PromoCell) supplemented with Myocyte Growth Medium supplement mix (C-39270, PromoCell).

AC16 and HPC cells were synchronized before each experiment by a 2-hour, 100 nM dexamethasone (Sigma-Aldrich, D4902) pulse (Balsalobre et al., 2000; van der Veen et al., 2012).

Reporter vectors, cell transfection and real time bioluminescence assays

The *BMAL1*-Luc and the *PER2*-Luc constructs suitable for real-time bioluminescence studies were obtained by cloning the corresponding human promoter regions. The *BMAL1* promoter region from -350 base pairs (bp) to + 100 bp relative to the gene transcriptional start site was inserted into red (pcBR) luciferase emitting vector (Promega, E1411). This DNA sequence deduced from previous report (Vollmers et al., 2008) starts 40 nucleotides before the CAAT box. The *PER2*-Luc vector was assembled with the human *PER2* promoter region from -480 bp to + 120 bp containing the minimal cycling promoter (Vatine et al., 2009) into a green luciferase vector (pcBG68, Promega, E1431). The pGL4.50 vector was purchased from Promega.

AC16 cells were batch-transfected with 10 µg reporter plasmid using Fugene HD transfection reagent (Promega, E2311) following the manufacturer's recommendations. Twenty-four hours after transfection, cells were split into 35 mm diameter dishes and incubated at 37°C, 5% CO₂ for 24 hours. Cells were synchronized by a 2h incubation with 100 nM dexamethasone. After a wash with 1x PBS, fresh medium containing 200 µM beetle luciferin potassium salt (Promega, E1601) was added onto cell layers and dishes were placed into a KRONOS AB-2550 luminometer (ATTO). Luciferase activities were measured for 1 min every 10 min under 5% CO₂ at 37°C for 4 days. Twenty hours after synchronization, bioluminescence monitoring was paused and HHT or vehicle was added to the cell culture medium. After a 4-hour treatment, cells were washed with 1x PBS and fresh medium containing luciferin (200 µM) was added. Signals were recorded as described above.

***In vitro* luciferase assay**

The purified recombinant luciferase (Promega, E2940) activity was determined *in vitro* as previously described (Berthier et al. 2021). The bioluminescence signal was quantified using a Victor Light Luminometer (PerkinElmer) in the presence of 0.1, 1 or 10 µM Luciferase Inhibitor II (Calbiochem, 119114) or of 0.1, 1 or 10 µM HHT.

***Ex vivo* luciferase activity monitoring**

Atrial tissue pieces were cultivated on inserts (Millicell 0.4 μ M, Millipore, PICMORG50) placed on 35 mm diameter plates containing 1.4 mL DMEM medium (Gibco, 31053) supplemented with 10% fetal calf serum, 10 mM HEPES, pH 7.4, 1% Glutamax, 1% penicillin-streptomycin cocktail and 200 μ M beetle luciferin potassium salt. Explants were then maintained at 36 °C with 5% CO₂ into a KRONOS-DIO AB-2550 (Atto) system. Luciferase signal was integrated for 1 min every 10 min during 1 week. The signal obtained was quantified and analyzed by the ATTO Dish type Luminescence Kronos software (version 2.30.243). Sinusoidal representation curves are detrended data generated by the software using temporal width set to \pm 12 h.

Rhythmic tests

Real time luciferase data were binned into 2-hour increments. Ex vivo luciferase data (heart explants) were first detrended using Kronos software as previously described (Martin-Burgos et al., 2022). Luciferase signals monitored before exposition to HHT or vehicle were removed prior statistical rhythmic tests. Data collected after the washout step were analyzed using Nitecap web application with default parameters (Brooks et al., 2022).

Protein extraction and Simple Western immunoassays

Cells were lysed using RIPA lysis buffer (10 mM TRIS-HCl, pH8.00, 1 mM EDTA , 0.5 mM EGTA , 140 mM NaCl, 1% Triton, 0.1% sodium deoxycholate, 0.1% SDS). Mouse heart proteins were extracted in the same buffer using a Minilys tissue homogenizer (Bertin Instruments) with 2.8 mm ceramic bead. The total protein amount was determined using the BCA method following manufacturer's recommendations (BCA protein assay kit, thermo scientific, 23227). REV-ERB α protein levels as well as loading control (HSP90 α / β or total protein) were analyzed by Simple Western[®] size-based or Total Protein assays using a Wes[®] system as recommended by the manufacturer (ProteinSimple). Proteins (0.5 mg/mL) were detected with primary antibodies described above. Secondary antibodies were provided by ProteinSimple (anti-Rabbit 042-206 or anti-mouse 042-205, ProteinSimple). Samples were processed according to manufacturer's recommendations. Data were analyzed using the Compass 6.1 software (ProteinSimple).

RNA extraction, microarray analysis and analogue drug identification

For microarray assays, AC16 cells were treated for 6 hours with 0.5 μ M digoxin (n=3), 1 μ M HHT (n=4) or corresponding vehicles (n=3). Briefly, RNA was purified using Nucleospin RNA columns (Macherey-Nagel) following manufacturer's recommendations. Total RNA amounts were determined by spectrophotometry using a Nanodrop One device (Thermo Scientific) and quality controls were performed using a RNA nano 6000 kit (Agilent) and a Bioanalyzer 2100 device (Agilent). Gene expression levels were determined using human Clariom S Arrays (Thermo Fisher Scientific, 902927) after RNA amplification, sscDNA labeling, and purification. Briefly, RNA was amplified using the GeneChip[™] WT PLUS Reagent Kit (Thermo Fisher Scientific, 902280), retro-transcribed to sscDNA and labeled using GeneChip[™] WT Terminal Labeling Kit (Thermo Fisher Scientific, 902281), followed by hybridization on the GeneChip human Clariom S30 Array (Thermo Fisher Scientific, 902917) according to the manufacturer's instructions. Raw data were processed using our in-house Galaxy instance "GIANT" (Galaxy-based interactive tools for Analysis of Transcriptomic data) (Vandel et al., 2020). Data has been deposited at the NCBI repository under the GEO number GSE222680 and

GSE222682. A LIMMA differential analysis was used to determine up- and down-regulated genes. Genes used for transcriptomic signature definition were selected with significant ($FDR \leq 0.05$) \log_2FC set between 1.2 and ≤ -0.8 or -1.2 for digoxin and HHT respectively. These thresholds were defined to limit the number of hits. Selected gene lists were analyzed using the L1000FWD tool to identify drugs with similar transcriptomic signatures using all cellular models available in the web application (Wang et al., 2018). Duplicated signatures have been merged while keeping the highest similarity score.

Statistics

Data were plotted as means \pm SEM. All statistical analyses were performed on all biological replicates using Prism (v 9.0, GraphPad Inc.). The number of biological replicates for each experiment has been detailed in corresponding figure legends. All groups were considered to have equal variances. For 2-group comparisons, a 2-sided Student's t-test was used. For multiple comparisons, a 1-way ANOVA followed by Dunnett's multiple comparison test or 2-way ANOVA followed by a Sidak's multiple comparisons test were applied as indicated in Figure legends. p values < 0.05 are considered as statistically significant.

Results

***In silico* identification of potential REV-ERB α proteostasis modulators.**

In agreement with our recent study (Vinod et al., 2022), we first confirmed that a 2h dexamethasone (dex) pulse synchronizes human AC16 cardiomyocytes revealing a time-dependent variation of total REV-ERB α protein amount, which showed a maximal expression 18-24 hours after synchronization (Fig. 1A). The expression of this nuclear receptor was totally inhibited by a 6h exposure to 0.5 μ M digoxin, a decrease which is abolished upon proteasome inhibition with Clasto-Lactacystin β -lactone (Vinod et al., 2022).

To identify drugs which could have a similar impact on REV-ERB α protein level as digoxin, transcriptomic data from digoxin-treated AC16 cells were leveraged to obtain a list of up- and downregulated genes (Fold Change < x-0.8 or > x1.2). This transcriptomic profile was then analyzed using the L1000FWD tool to compare the digoxin-modulated gene pattern in AC16 cells with those induced by more than 16,000 compounds on a pool of cancer cell lines (Wang et al., 2018). Reassuringly, this analysis detected several perturbationagens transcriptionally acting similar as digoxin which were structurally close cardiotonic steroids (cinobufagin, bufalin, ouabain...) (Fig. 1C and Sup Table 1). Another prominent chemical class was small molecules with potent protein synthesis inhibitory properties, such as anisomycin, narciclasine and cephaeline (Tan et al., 1991; Dmitriev et al., 2020). Interestingly, anisomycin has already been described as a circadian modulator (Watanabe et al., 1995), further validating approach.

Time and dose-dependent effect of homoharringtonine on REV-ERB α protein level.

We noted a similarity score (88% of the digoxin-like score) for the anti-cancer compound homoharringtonine (HHT) which exerts its beneficial anti-leukemic activity by binding to ribosomes, thereby disabling the elongation of nascent peptide chains (Tujebajeva et al., 1989). As this FDA-approved anti-cancer drug is associated with cardiovascular complications (Kantarjian et al., 2013) and also has anti-fibrotic properties in heart (Kreutzer et al., 2022), it prompted us to further characterize HHT activity on REV-ERB α protein expression in cardiomyocytes.

To do so, AC16 cells were synchronized and treated for 24h with increasing concentrations of HHT, from 0.1 μ M to 10 μ M. In these conditions, REV-ERB α protein content was reduced by 37% with 0.1 μ M HHT and was undetectable from 1 μ M HHT (Fig. 2A). Since the digoxin-dependent REV-ERB α degradation is significant within 6h (or less) of treatment [Fig. 1B and (Vinod et al., 2022)], the effect of a shorter exposure to HHT was also tested. Here again, 4h of treatment were enough to reduce the protein amount even with the lowest dose of HHT (Fig. 2B). To assess whether HHT does not act only on cancer/transformed cells, synchronized human primary cardiomyocytes were treated for 4h (from 20h to 24h post-synchronization) with 1 μ M HHT (Fig. 2C). Again, HHT totally blunted REV-ERB α protein expression, suggesting that its mechanism of action is not specific to transformed cells.

So far, whether HHT can target cardiac REV-ERB α protein *in vivo* has not been investigated. To address this, a single dose of HHT was injected intraperitoneally (1 mg/kg) in mice at ZT5, i.e. 4h before the REV-ERB α protein zenith [ZT9, (Vinod et al., 2022)]. Lu and colleagues have previously shown that HHT is able to reach the cardiac tissue from the dog and that 1% of the dose is still present in the organ 5h after i.v. femoral injection (Lu et al., 1988). The clinical dose recommended

for human is 2 injections of 1.25 mg/m²/day. Thus, for an individual of 175 cm for 70 kg, the body surface correspond to 1.85 m² and the admitted dose is 4.625 mg/days or 0.07mg/kg. The dose administrated to animal in our study (1 mg/kg) is based on literature (Li et al., 2020; Wang et al., 2021) and is 15-fold higher than the human clinical recommendation, and 4-fold below the toxic dose in mouse (Yakhni et al., 2019). Under our conditions, this alkaloid reduced REV-ERB α protein level by more than 20 % at ZT9, its usual peak time in mouse hearts (Fig. 2D). Taken together, our data show that the protein synthesis inhibitor HHT interferes with REV-ERB α protein level both *in vitro* and *in vivo*. To decipher the specificity of HHT on REV-ERB α proteostasis, BMAL1 and CLOCK protein levels were determined after a 6-hour exposition to the drug. Contrasting with REV-ERB α , both transcription factors were stabilized in presence of HHT (Fig. 2E).

Effects of protein synthesis inhibitors on REV-ERB α protein level.

From a mechanistic point of view, our results also suggested that cellular REV-ERB α protein content, mostly known to be regulated through the ubiquitin-proteasome pathway (Zhao et al., 2016), is also significantly regulated through its synthesis rate. Since protein translation inhibitors may interfere with the activity of many components of the translational machinery (Fan and Sharp, 2021), we aimed at identifying compounds acting upstream of the elongation step and affecting REV-ERB α protein synthesis. A transcriptomic analysis was first performed on synchronized AC16 cells treated for 4h with 1 μ M HHT to map the transcriptional blueprint of HHT against the LINCS L1000 database using the L1000FWD tool as above. In order to improve the stringency of the analysis, up- and downregulated gene fold change (FC) threshold was set to absolute Log₂ FC>1.2 (FDR \leq 0.05). As expected, HHT itself was identified by this analysis, together with a significant number of protein synthesis inhibitors such as anisomycin, cephaeline and narciclasine, which were also identified as “digoxin-like” molecules (Sup Table 1). The 50 top hits from each L1000 analysis (digoxin and HHT) were compared to identify compounds potentially acting with a similar mechanism of action. This *in silico* screening allowed the identification of digoxin structural analogues (bufalin and ouabain) and of several protein synthesis inhibitors (Fig. 3). Other types of anti-cancer drugs such as clofarabine, obatoclax and others with seemingly distinct mechanisms of action were also identified by this approach (Fig. 3 and Sup table 1).

We then validated this *in silico* approach by testing a panel of 7 of these molecules for their ability to alter REV-ERB α protein level in synchronized AC16 cells. In addition to the proteasomal activators bufalin and ouabain which were previously demonstrated to funnel REV-ERB α to the proteasome (Vinod et al., 2022), 3 out of 3 tested molecules classified as protein synthesis inhibitors were active in our REV-ERB α proteostasis assay [cephaeline, narciclasine and verrucaric acid (Sup_Fig. 1B and 1C)]. With the exceptions of the survivin inhibitor YM-155 (Nakahara et al., 2007) and the bone morphogenetic protein (BMP) signaling inhibitor LDN-193189 (Cuny et al., 2008), none of the other compounds was active in AC16 cells (Sup_Fig. 1B and 1C). This demonstrated that an essential arm of REV-ERB α proteostasis regulation is the protein translation process. Of note, all tested protein synthesis inhibitors act at late steps of this process, mostly at the peptidyl transferase reaction (Fig. 4).

To gain further insights into steps required for efficient REV-ERB α translation, we further tested inhibitors acting upstream of the elongation step (Fig. 4). Our previous work ruled out a contribution of the mTOR pathway in our system (Vinod et al., 2022). Compounds interfering with initiation steps such as compounds preventing eIF4E binding to eIF4G (4-EG11), interfering with eIF4A helicase activity (rocaglamide, silvestrol, CR-1-31-B), or preventing 80S initiation complex formation

(salubralin) were tested (Fig. 4). Puromycin was tested as a widely-used molecule representative of elongation inhibitors. In the AC16 cell model, 4-EGI1 had no effect on REV-ERB α (Sup_Fig. 1F), in opposition to its impact on REV-ERB α protein levels in synchronized U2OS cells (data not shown). All other translation inhibitors strongly reduced REV-ERB α protein amount (Sup_Fig. 1C, 1D and 1F). In parallel, we assessed whether the upstream ORF (uORF) located upstream of the *NR1D1* locus encoding REV-ERB α (Janich et al., 2015) could have a functional importance in regulating cardiomyocytic REV-ERB α protein levels. uORFs generally have an inhibitory role on protein translation by blocking ribosome processivity, and thwarted translation at downstream CDS can be relieved using ISRIB (integrated stress response inhibitor), a small molecule inhibitor of the eIF2 α kinase (Young and Wek, 2016). ISRIB alone had no effect on REV-ERB α protein level, and was also inefficient at restoring its synthesis in presence of HHT (Sup_Fig. 1F). Finally, treatment with the SRC activator MCB-613, able to induce eIF2 α phosphorylation (Wang et al., 2015), clearly reduced REV-ERB α protein level (Sup_Fig. 1E). Thus, all tested protein synthesis inhibitors except 4-EGI1, irrespective of their mechanism of action, strongly impact REV-ERB α protein production in cardiomyocytes. Moreover, the *NR1D1* uORF is not operative in our cardiomyocyte cellular model.

Protein synthesis inhibition by HHT affects the cellular circadian clock.

Since a single administration of these drugs affected cardiac REV-ERB α proteostasis, we determined whether this nuclear receptor is the only component of the clock machinery to be affected by these perturbagens. HHT was used as a reference compound to determine potential global effects on the clock machinery. CCG mRNA expression levels in 4h HHT-treated synchronized AC16 cells were determined (24h after synchronization) by microarray analysis. Most of them were upregulated with the exception of *PER3*, *CLOCK*, *RORA* and *RORC* (Fig. 5A). *REV-ERB α /NR1D1* and its target genes *ARNTL1/BMAL1*, *NR1D2*, *CDKN1A* and *NFIL3* were upregulated in agreement with the loss of REV-ERB α protein expression. Surprisingly, the other CCGs such as *PER1/2* and *CRY1/2* were also upregulated (Fig. 5A). This was suggestive of a more general impact of HHT on circadian TTFLs, which was explored by real-time monitoring of *BMAL1* and *PER2* promoter activities. For this purpose, *BMAL1* and *PER2* promoters hooked to a luciferase gene were transfected in AC16 cells, from which luciferase activity was continuously recorded for several days. Prior to running these assays, we first assessed whether HHT interferes directly with luciferase enzymatic activity, as this is a major source for false positive detection in luciferase-based screening procedures (Berthier et al., 2021). The activity of purified recombinant luciferase enzyme was determined in presence of varying concentrations of HHT or of a specific luciferase inhibitor as a positive control. In contrast to the Luc inhibitor, HHT did not significantly modify recombinant luciferase activity even at high concentrations (Fig. 5B). Twenty hours after synchronization, transfected cells were treated for 4h with increasing concentrations of HHT. During the 4h treatment, the luciferase activity was transiently reduced in a dose-dependent manner in both models (Fig. 5C). To understand the apparent contradiction between the observed upregulation of endogenous gene expression (Fig. 5A) and downregulation of exogenous reporter activities, AC16 cells were transfected with a luciferase vector controlled by a highly constitutively active cytomegalovirus (CMV) promoter. When synchronized cells were treated for 4 h with 1 μ M HHT, the bioluminescence signal decreased by about 50% (Sup_Fig. 2). The half-life of the firefly luciferase protein being \approx 3 to 4 hours (Leclerc et al., 2000), this reduction of signal clearly indicated an inhibition of luciferase synthesis. Thus, the bioluminescence signal reduction observed with *BMAL1* or *PER2* promoter models did not reflect an alteration of promoter activities but a reduction of the luciferase mRNA translation. While these reporter models were not fully adequate to study the effect of HHT on the circadian machinery, we nevertheless noted that

transient exposure to HHT was compatible with a recovery of BMAL1 or PER2 promoter activities. JTK_cycle analysis of data confirmed that rhythmicity was maintained in all conditions (Bmal-luc q-values ≤ 0.008 , Per2-Luc q-values ≤ 0.03). HHT clearly reduced the amplitude and induced a phase shift to the right in a dose-dependent manner, without impacting the period of these oscillations. We note that the phase shift was more pronounced for the Per2-Luc signal (from 2.9h to 4.5h) compared to the Bmal1-Luc signal (1.16 to 1.9 h). Cells were exposed to HHT 20 h after synchronization, thus when *Bmal1* expression decreases, and when *Per2* expression increases. We speculate that this observed differential phase shift results from distinct interference with multiple time-dependent processes regulating protein stability (Fig. 5C).

To further investigate a potential global alteration of the cardiac clock machinery during HHT therapy, we used an alternative *ex vivo* model based on the monitoring of a transgenic PER2::LUC fusion protein to directly interrogate endogenous PER2 protein level via the activity of the luciferase moiety activity (Yoo et al., 2004). Atrial explants from PER2::LUC mice were transiently exposed to 100 nM HHT for 24h, while luciferase activity was recorded in real-time for several days before and after treatment. HHT transiently blunted PER2::LUC fusion protein bioluminescent signal (data not shown). After wash out, PER2::LUC fusion protein recovered a cyclic, circadian activity (JTK-cycle analysis: DMSO (vehicle) q value = 0.002, HHT q value = $7.5e^{-11}$) with a marked 12h phase shift to the right which was stable over time (Fig. 5D). Taken together, these observations suggest that even a transient interference with protein synthesis may propagate long-lasting effects on circadian rhythmicity. In addition, PER2::LUC signals were delayed by 13.4 h (± 1.9 h), suggesting that this translation inhibition-induced phase shift is probably due to the HHT-dependent resetting of the cardiac circadian clock (Fig. 5D).

Conclusion

Knowing the interconnection between the clock machinery and main body functions, e.g. metabolic, cardiovascular and immune regulations, a regular and synchronously paced circadian rhythm in all organs is required for the preservation of physiological homeostasis. Several groups have shown that protein synthesis inhibitors such as cycloheximide and anisomycin were able to affect the circadian rhythm (Jacklet, 1977; Olesiak et al., 1987; Watanabe et al., 1995). However, this concept has been set aside to focus mostly on the equilibrium between mRNA synthesis and degradation of both transcripts and proteins to explain the cyclicity of the circadian regulations (Dibner et al., 2009; Westermarck and Herzog, 2013; Luck et al., 2014; Vinod et al., 2022). Here we show that controlling protein translation at various steps severely affected REV-ERB α proteostasis in particular and the molecular clock in general. While this observation may seem trivial at first, we note that potential iatrogenic effects resulting from a prolonged exposure of patients to these compounds affecting the circadian rhythm are not considered. Second, the use of these quite common reagents such as puromycin in biological experiments may significantly affect circadian rhythm-controlled biological responses and generate confounding effects which are not integrated in data analysis. Finally, we note that protein translation is itself cyclic and connected to circadian regulatory processes (Atger et al., 2015; Sinturel et al., 2017; Castillo et al., 2022), highlighting a complex connection between protein translation control and the molecular clock. Nevertheless, to our knowledge no recent investigation has been developed to analyze the effect of protein synthesis inhibitors on the circadian clock itself.

In addition to its selective cytotoxicity on cancer cells through SRC coactivator “super-activation” (Wang et al., 2015; Bazzaro and Linder, 2020), MCB-613 has cardioprotective effects post-myocardial infarction (Mullany et al., 2020). We previously demonstrated that the reduction of REV-ERB α activity or of protein amount improved recovery of the heart after an ischemia/reperfusion episode (Montaigne et al., 2018; Vinod et al., 2022). Therefore, it can be hypothesized that part of MCB-613’s cardioprotective effect stems from its ability to blunt REV-ERB α protein synthesis. Similarly, narciclasine (a.k.a. lycoricidinol), an anticancer alkaloid structurally unrelated to MCB-613, but also reducing REV-ERB α protein level, also shows cardioprotective properties after acute myocardial injury (Tang et al., 2021).

The (potential) use of protein synthesis inhibitors in cancer may be extended to other pathologies caused by fungi, parasites and viruses including SARS-CoV2 (Choy et al., 2020; Muller et al., 2021; Shahid and Shahzad-UI-Hussan, 2021). Enlarging their spectrum of therapeutically applications has prompted many clinical evaluations in distinct pathologies, on the sole basis of their ability to reprogram cellular translationalomes. As an example, eIF4A inhibitors (e.g. rocaglates) are powerful CAP-dependent translational inhibitors and their entry into clinical evaluation relies mostly on this property. However, cytotoxic effects of rocaglates are much more complex and involve signaling pathways activation (Ho et al., 2021). Our data highlight unsuspected effects of rocaglates and other translational inhibitors on circadian rhythm, thereby potentially affecting numerous biological processes such as metabolism, heart and muscle physiology.

Finally, we note that transient HHT treatment induced a long-lasting circadian rhythm phase shift. Therefore, depending on the relative bioavailability of this and of other tested compounds, this raises the possibility of drug-induced organ(s)-specific circadian phase shift and pathological outcomes. The effect observed on the heart in this study should encourage further investigation of possible consequences on other organs. Indeed, tissue-selective disruption of molecular clock components may have severe effects on behavior, cardiac physiology and metabolic homeostasis (Guan and Lazar, 2021), calling for a careful investigation of core molecular clock component levels

during and after administration of translational inhibitors, as other Zeitgebers such as food or light may restore or not the clock when the drug is cleared off the organ.

Acknowledgments

This work was supported by grants from INSERM, Région Hauts de-France and Université de Lille (START'AIRR REV-ERBalpha/SAS20215), LABX EGID (ANR-10-LABX-0046). MJ is supported by a Bourse d'excellence Wallonie-Bruxelles International (WBI) World (ref. SOR/2019/441207) and a Sheila Sherlock fellowship from the European Association for the Study of Liver (EASL). BS is a recipient of an Advanced ERC Grant (694717).

Author contributions

Conceptualization: AB, JE, PL, BS; Experimentation: AB, CG, MJ, MV; Writing: AB, PL; Funding acquisition: PL, BS.

Declaration of Conflicting Interests

The authors declare that there is no conflict of interest.

Figures and legends

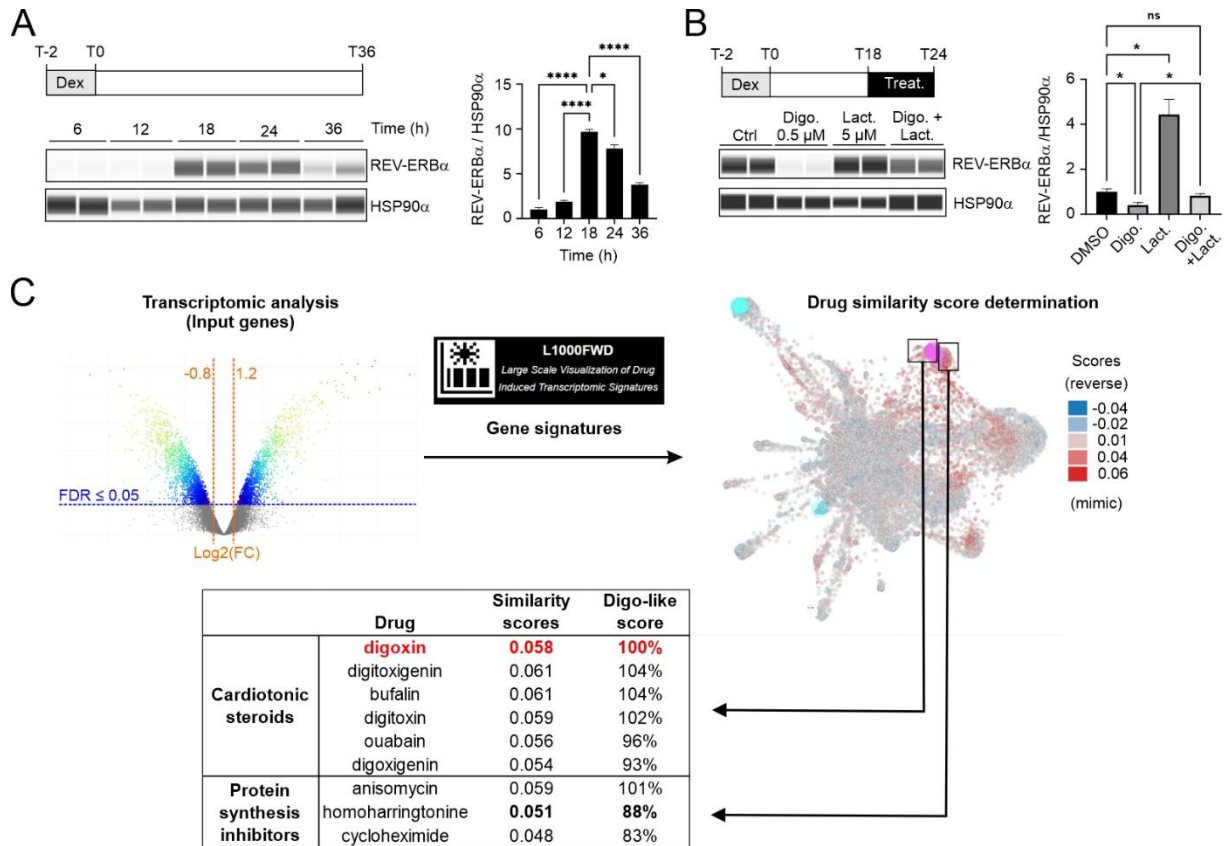


Figure 1: Identification of digoxin transcriptional similars. **A:** Time course of REV-ERB α protein level variations (n=2). Upper left panel: experimental scheme. Dex: dexamethasone. Lower left panel: REV-ERB α protein fluctuations over time were determined by WES analysis of whole cell extracts from synchronized AC16. Right panel: densitometric analysis of WES data. Data were normalized to HSP90 α content. **B:** Digoxin (Digo.) effect on REV-ERB α protein levels. Upper left panel: experimental scheme. Dex: dexamethasone, Lact.: Clasto-Lactacystin β -lactone. Lower left panel: WES analysis of REV-ERB α protein level in synchronized AC16 cells, treated for 6h with 0.5 μ M digoxin (n=2), 5 μ M Clasto-Lactacystin β -lactone (n=2), both drugs (n=2) or vehicle control (n=2). Right panel: densitometric analysis of WES data. Data were normalized to HSP90 α content. Results are expressed as mean \pm SEM and values were compared by a one-way ANOVA followed by a Dunnett post hoc test (**A**) or a Brown-Forsythe and Welch ANOVA tests (**B**). *p<0.05, **p<0.01 and ****p<0.0001. Data shown are a representative experiment performed in duplicate. **C:** Transcriptional similarities of digoxin treatment compared to the L1000 database. The transcriptomic profile of AC16 cells treated with digoxin (0.5 μ M, 6h) was determined by microarray analysis and a signature similarity search was performed using L1000FWD. Left panel: Clustering of gene signatures and mapping of digoxin-like molecules. Right panel: top hits as determined by the L1000FWD algorithm. The similarity score is the overlap between the input up/down genes and the signature up/down genes divided by the effective input (Wang et al., 2018). The Digo-like score is the similarity score divided by the digoxin similarity score multiplied by 100.

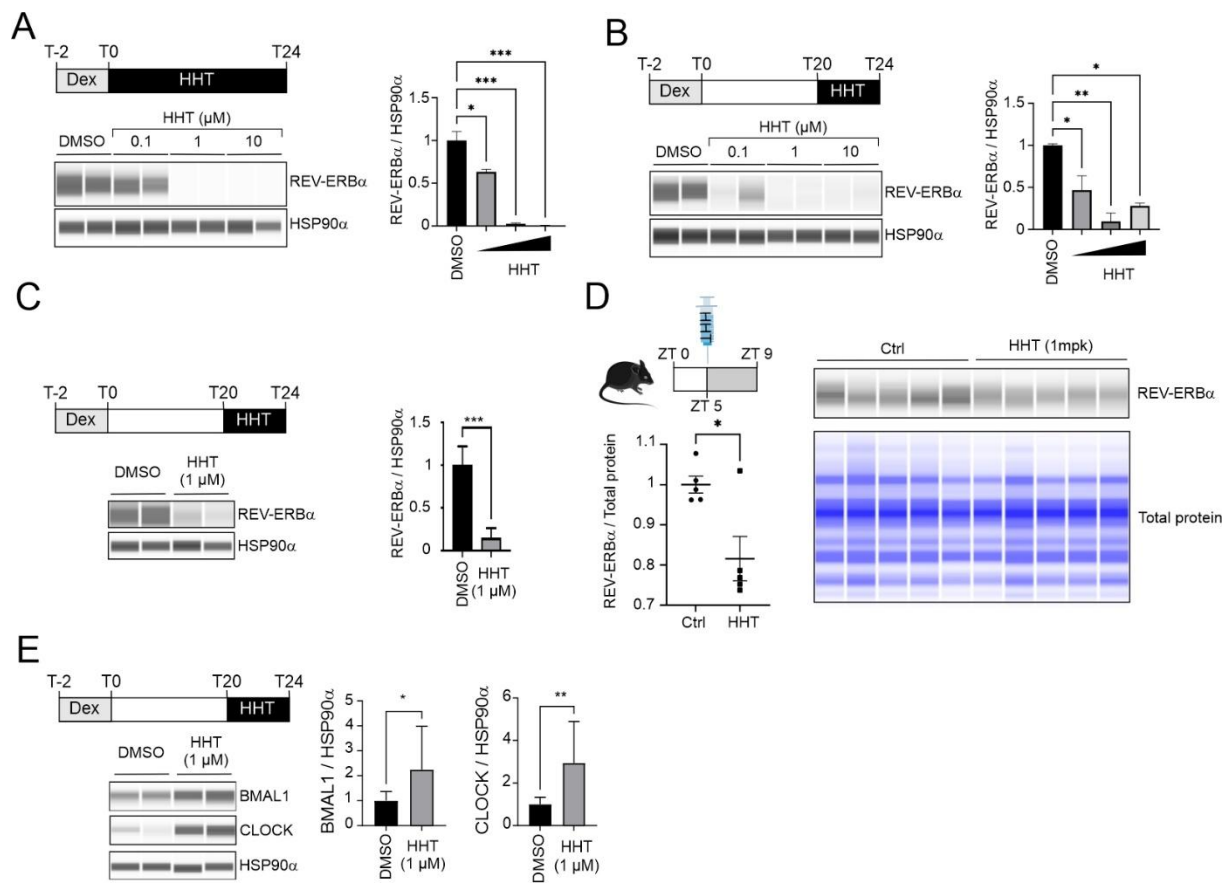


Figure 2: Effect of HHT on REV-ERB α protein level *in vitro* and *in vivo*. **A:** Dose-dependent effect of HHT on REV-ERB α protein levels in AC16 cells. Upper left panel: experimental scheme. Dex: dexamethasone. Lower left panel: REV-ERB α protein levels were determined by WES analysis of synchronized AC16 whole cell extracts. Right panel: densitometric analysis of WES data. Data were normalized to HSP90 α content. **B:** Dose-dependent effect of HHT (short treatment) on REV-ERB α protein levels in AC16 cells. Upper left panel: experimental scheme. Dex: dexamethasone. Lower left panel: REV-ERB α protein levels were determined by WES analysis of synchronized AC16 whole cell extracts. Right panel: densitometric analysis of WES data. Data were normalized to HSP90 α content. **C:** Effect of HHT (short treatment) on REV-ERB α protein levels in human primary cardiomyocytes. Upper left panel: experimental scheme. Dex: dexamethasone. Lower left panel: REV-ERB α protein levels were determined by WES analysis of whole cell extracts from synchronized human primary cardiomyocyte. Right panel: densitometric analysis of WES data. Data were normalized to HSP90 α content. **D:** Effect of HHT REV-ERB α levels in mouse heart. Upper left panel: experimental scheme. HHT was injected at ZT5, *i.e.* 4h prior to the REV-ERB α protein peak. Hearts were collected at ZT9. Right panel: REV-ERB α protein levels were determined by WES analysis of whole heart extracts. Lower left panel: densitometric analysis of WES data. Data were normalized to total protein content as determined by WES analysis. **E:** Effect of HHT (short treatment) on BMAL1 and CLOCK protein levels in AC16. Upper left panel: experimental scheme. Dex: dexamethasone. Lower left panel: REV-ERB α protein levels were determined by WES analysis of whole cell extracts from synchronized human primary cardiomyocyte. Right panel: densitometric analysis of WES data. Data were normalized to HSP90 α content. Results are expressed as mean \pm SEM (A, B, C, D and E). Values were compared by a one-way ANOVA followed by a Dunnett post hoc test (A, B and E) or a t test (C and D). * $p < 0.05$, ** $p < 0.01$ and *** $p < 0.001$. Data correspond to a representative experiment

with biological replicates (n=2 for A, B, C, E, or n=5 for D) reproduced twice (A, B and C) or 3 times independently (E).

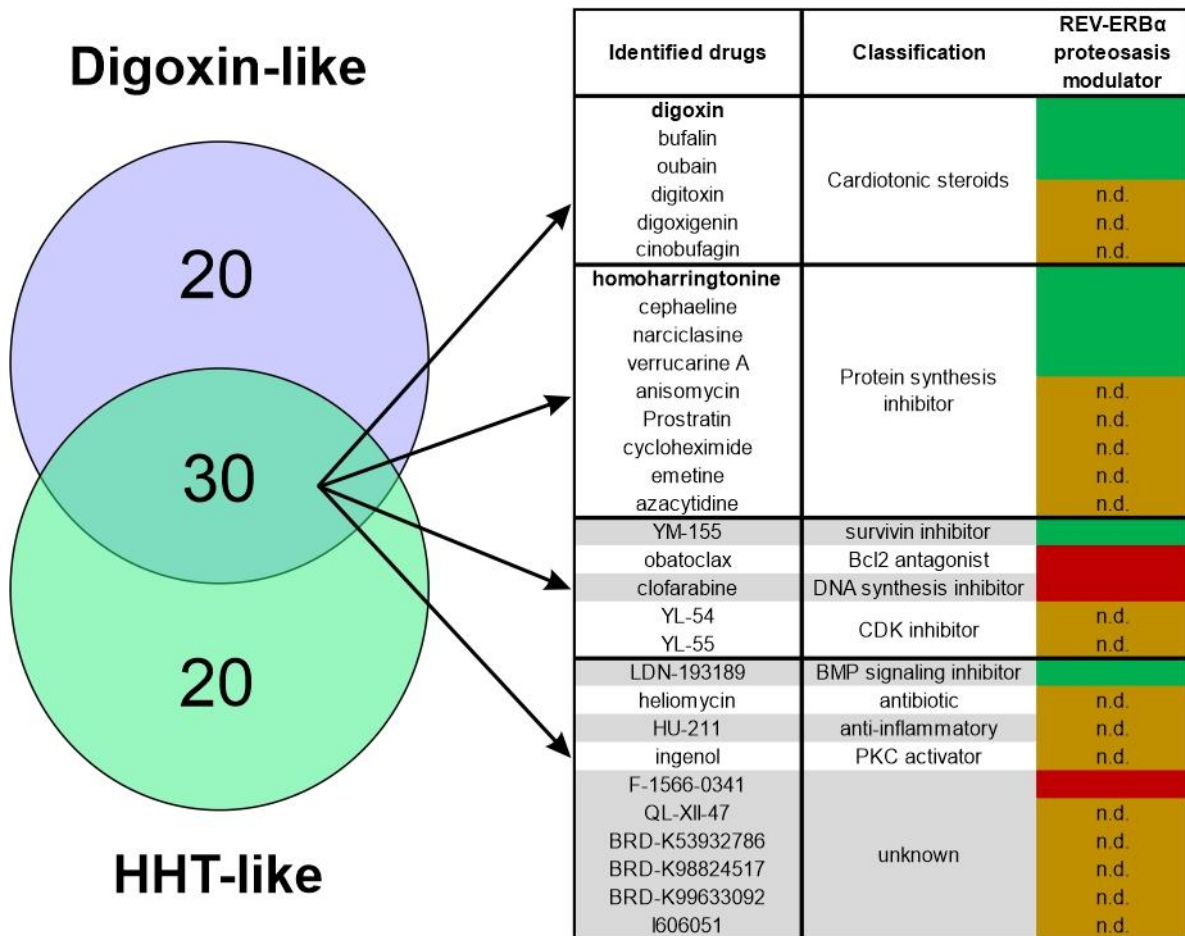


Figure 3: Identification of drugs having a transcriptional signature close to that of digoxin and HHT. Digoxin and HHT transcriptional similars were identified using L1000FWD. The top 50 hits from each list were crossed to identify molecules having potentially similar effects on REV-ERB α protein levels. The 30 identified common drugs (right panel) are classified according to their known targets/mechanism of action. n.d.: not determined; green: triggers REV-ERB α protein level decrease; red: no effect on REV-ERB α protein level.

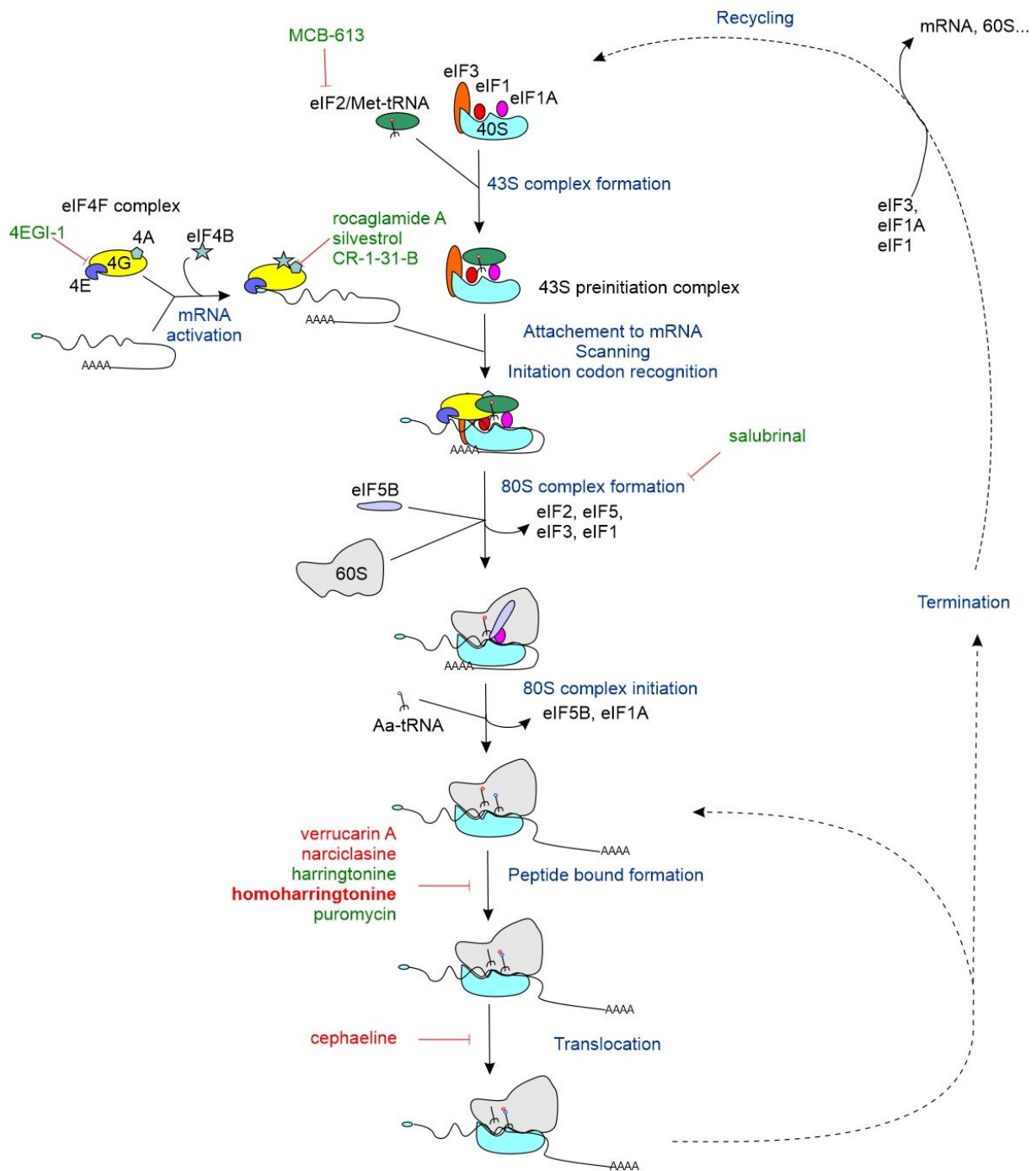


Figure 4: Overview of the protein synthesis pathway [adapted from (Jackson et al., 2010; Wang et al., 2015; Dmitriev et al., 2020)]. *In silico* identified (in red) or manually selected (in green) translation inhibitors affecting REV-ERB α protein level are indicated on the graph.

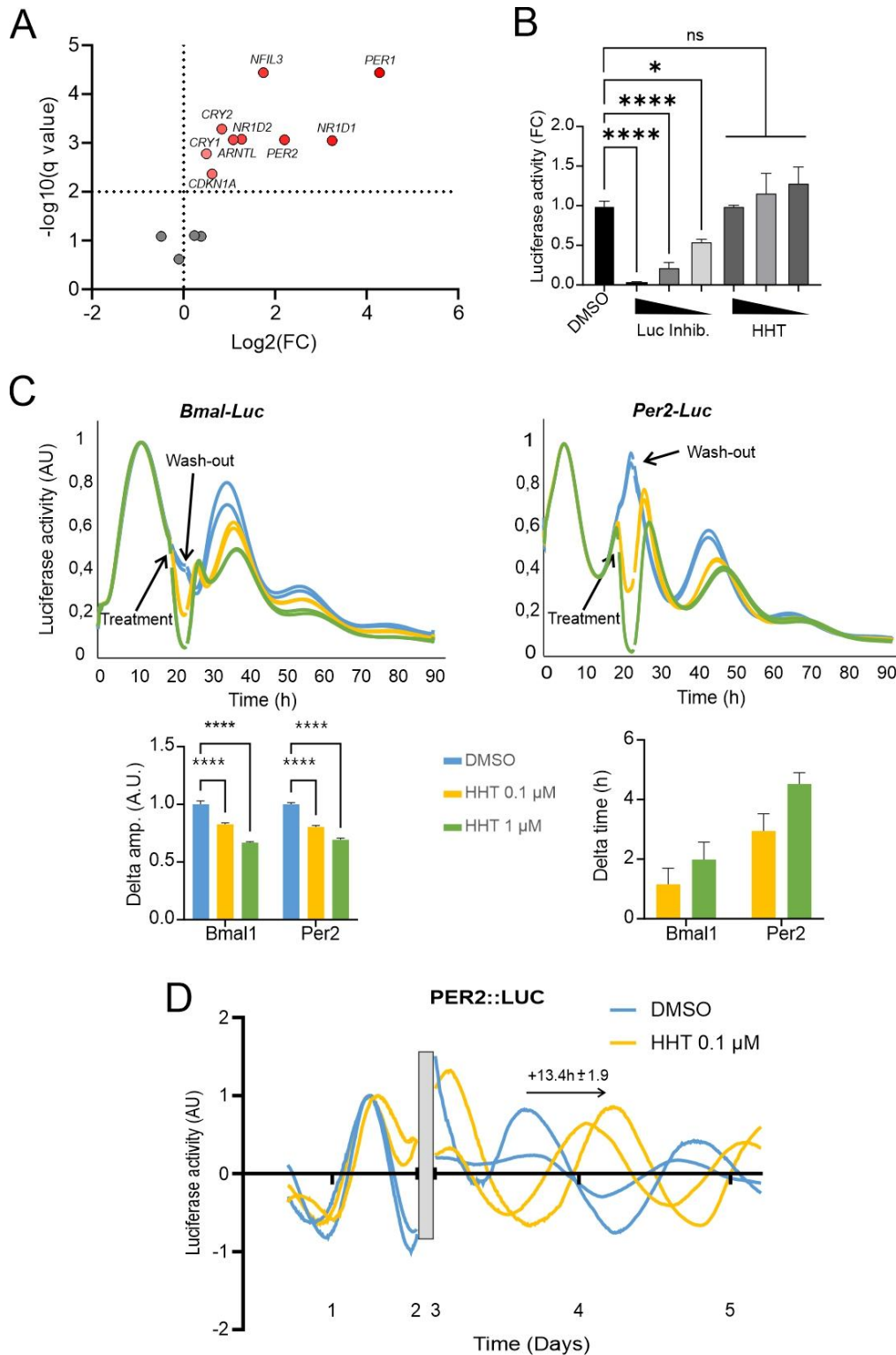
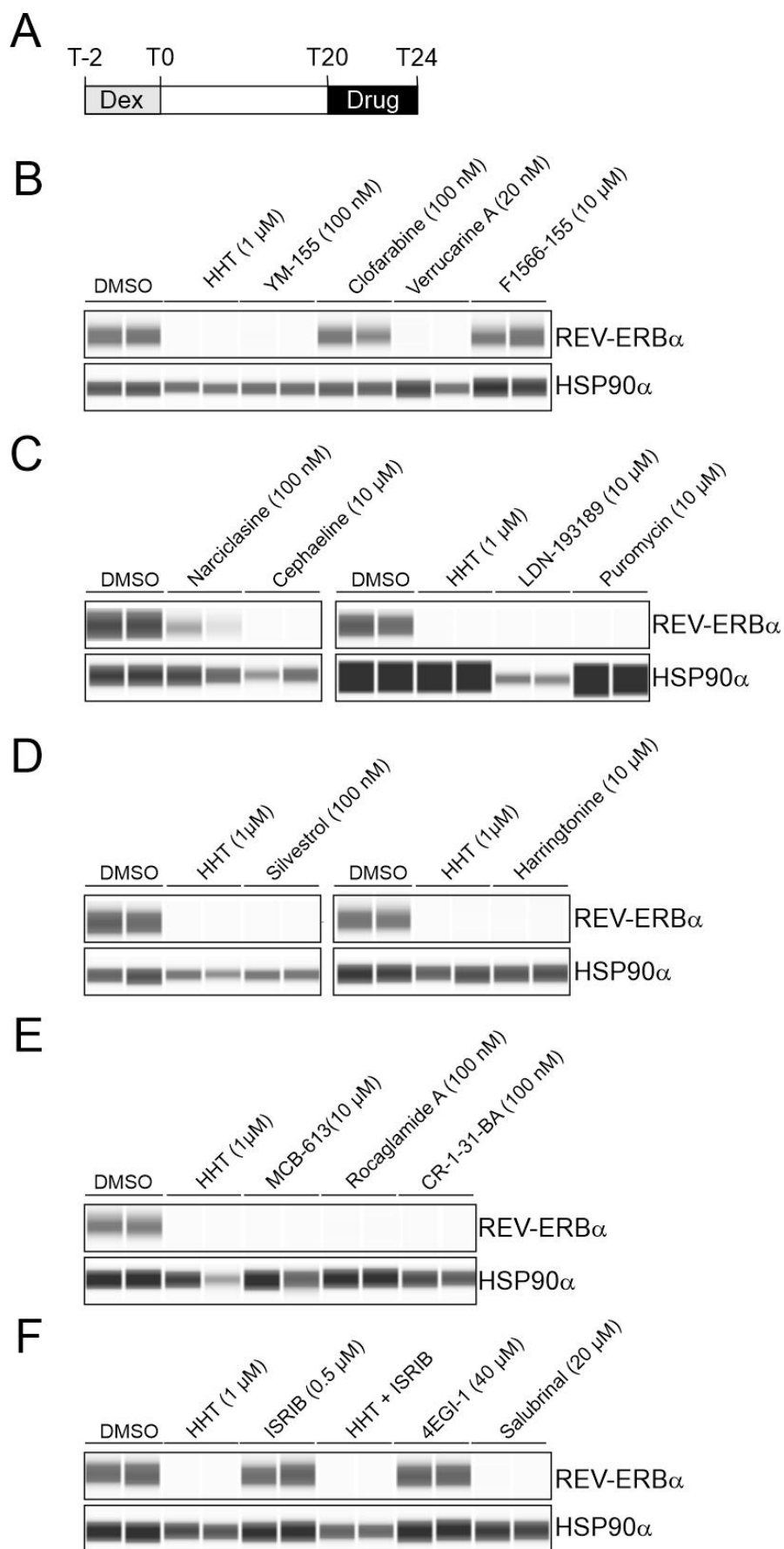


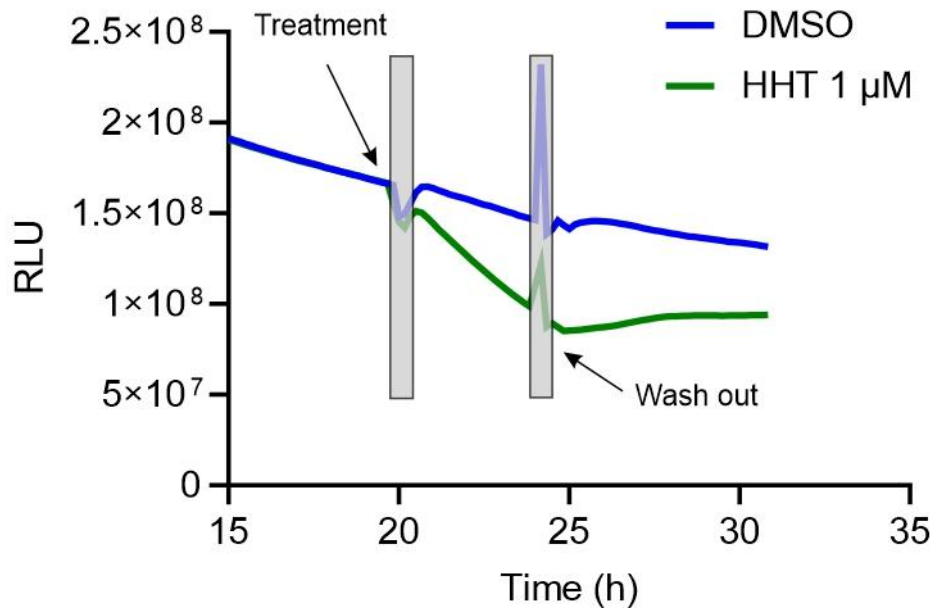
Figure 5: The clock machinery is disrupted by HHT. **A:** Volcano plot of normalized CCGs expression fold change in synchronized AC16 cells and after a 4h treatment (n=4) or not (n=3) by HHT. Cells were exposed to the drug 20 hours after synchronization. Statistical significance was determined by multiple unpaired t tests with a False Discovery Rate (FDR) set to 0.01. **B:** *In vitro* recombinant luciferase activity assay (n=3) in the presence of increasing doses of luciferase inhibitor II or HHT (0.1μM, 1μM, 10μM). Results are expressed as mean ± SEM and values were compared by a one-way ANOVA followed by a Dunnett post hoc test. *p<0.05 and ****p<0.0001 (ns= non significant). **C:** Real time luciferase reporter activity. AC16 cells were transfected by the indicated reporter gene and

Luciferase activity was monitored. Twenty hours after synchronization, cells were treated for 4h with vehicle or increasing doses of HHT then washed out 4 hours later. Curves shown representative signal of 2 biological replicates for each conditions. Histograms correspond to the variation in signal amplitude compared to DMSO (Delta amp.) and the shift compared to control condition (DMSO) at zeniths (Delta time) for 2 independent experiments processed in duplicate (n=4). Statistical significance was determined by a 2-way ANOVA followed by a Sidak's multiple comparisons test (****p<0.0001). **D:** Ex vivo Per2::Luc fusion protein activity in transgenic mouse atrial explants. After collection of hearts, the luciferase activity was monitored in real-time for 2 days from isolated heart explants. Explants were then treated (n=2) or not (n=2) for 24h with 0.1 μ M HHT then washed out as above. Signals was presented as detrended data. The gray box indicates the treatment window. Within this interval, curves have been removed to mask system opening and fresh luciferase addition generated optical artifacts non-standardizable between the 2 independent experiments.



Berthier et al., Supp Figure 1

Supplemental Figure 1: Effect of digoxin and HHT similars on REV-ERB α protein expression. A: Experimental scheme. AC16 cells were plated and synchronized with dexamethasone for 2 hours. Twenty hours later, cells were treated with compounds for 4 hours and cell lysates were assayed for their content in REV-ERB α protein and HSP90 α as a loading control. **B-F:** WES analysis of REV-ERB α protein levels after a 4 hour-treatment with the indicated compounds. Presented data correspond to a representative experiment processed in duplicates. Results has been confirmed with a replicated experiment.



Berthier et al., Supp Figure 2

Supplemental Figure 2: HHT effect on cellular luciferase accumulation. AC16 cells were transfected with a luciferase reporter gene driven by the constitutive CMV (cytomegalovirus) promoter. Light emitted by transfected and synchronized cells, treated or not with 1 μ M HHT, was monitored for 35 hours. Gray boxes indicate moments of treatment and wash out.

Supplemental Table 1: List of drugs presenting a digoxin- or HHT-like treated synchronized AC16 cells transcriptional profile (<https://figshare.com/s/042e1cae295429eeaf4d>).

References

- Atger F, Gobet C, Marquis J, Martin E, Wang J, Weger B, Lefebvre G, Descombes P, Naef F, and Gachon F (2015) Circadian and feeding rhythms differentially affect rhythmic mRNA transcription and translation in mouse liver. *Proc Natl Acad Sci U S A* 112:E6579-6588.
- Balsalobre A, Brown SA, Marcacci L, Tronche F, Kellendonk C, Reichardt HM, Schutz G, and Schibler U (2000) Resetting of circadian time in peripheral tissues by glucocorticoid signaling. *Science* 289:2344-2347.
- Baron KG, and Reid KJ (2014) Circadian misalignment and health. *Int Rev Psychiatry* 26:139-154.
- Bazzaro M, and Linder S (2020) Dienone Compounds: Targets and Pharmacological Responses. *J Med Chem* 63:15075-15093.
- Berthier A, Staels B, and Lefebvre P (2021) An optimized protocol with a stepwise approach to identify specific nuclear receptor ligands from cultured mammalian cells. *STAR Protoc* 2:100658.
- Brooks TG, Mrcela A, Lahens NF, Paschos GK, Grosser T, Skarke C, FitzGerald GA, and Grant GR (2022) Nitecap: An Exploratory Circadian Analysis Web Application. *J Biol Rhythms* 37:43-52.
- Castillo KD, Wu C, Ding Z, Lopez-Garcia OK, Rowlinson E, Sachs MS, and Bell-Pedersen D (2022) A circadian clock translational control mechanism targets specific mRNAs to cytoplasmic messenger ribonucleoprotein granules. *Cell Rep* 41:111879.
- Choy KT, Wong AY, Kaewpreedee P, Sia SF, Chen D, Hui KPY, Chu DKW, Chan MCW, Cheung PP, Huang X, Peiris M, and Yen HL (2020) Remdesivir, lopinavir, emetine, and homoharringtonine inhibit SARS-CoV-2 replication in vitro. *Antiviral Res* 178:104786.
- Cuny GD, Yu PB, Laha JK, Xing X, Liu JF, Lai CS, Deng DY, Sachidanandan C, Bloch KD, and Peterson RT (2008) Structure-activity relationship study of bone morphogenetic protein (BMP) signaling inhibitors. *Bioorg Med Chem Lett* 18:4388-4392.
- de Assis LVM, and Oster H (2021) The circadian clock and metabolic homeostasis: entangled networks. *Cell Mol Life Sci* 78:4563-4587.
- Dibner C, Sage D, Unser M, Bauer C, d'Eysmond T, Naef F, and Schibler U (2009) Circadian gene expression is resilient to large fluctuations in overall transcription rates. *EMBO J* 28:123-134.
- Dmitriev SE, Vladimirov DO, and Lashkevich KA (2020) A Quick Guide to Small-Molecule Inhibitors of Eukaryotic Protein Synthesis. *Biochemistry (Mosc)* 85:1389-1421.
- Elbaz HA, Stueckle TA, Tse W, Rojanasakul Y, and Dinu CZ (2012a) Digitoxin and its analogs as novel cancer therapeutics. *Exp Hematol Oncol* 1:4.
- Elbaz HA, Stueckle TA, Wang HY, O'Doherty GA, Lowry DT, Sargent LM, Wang L, Dinu CZ, and Rojanasakul Y (2012b) Digitoxin and a synthetic monosaccharide analog inhibit cell viability in lung cancer cells. *Toxicol Appl Pharmacol* 258:51-60.
- Fagiani F, Di Marino D, Romagnoli A, Travelli C, Voltan D, Di Cesare Mannelli L, Racchi M, Govoni S, and Lanni C (2022) Molecular regulations of circadian rhythm and implications for physiology and diseases. *Signal Transduct Target Ther* 7:41.
- Fan A, and Sharp PP (2021) Inhibitors of Eukaryotic Translational Machinery as Therapeutic Agents. *J Med Chem* 64:2436-2465.
- Guan D, and Lazar MA (2021) Interconnections between circadian clocks and metabolism. *J Clin Invest* 131.
- Herrmann J (2020) Adverse cardiac effects of cancer therapies: cardiotoxicity and arrhythmia. *Nat Rev Cardiol* 17:474-502.
- Ho JJD, Cunningham TA, Manara P, Coughlin CA, Arumov A, Roberts ER, Osteen A, Kumar P, Bilbao D, Krieger JR, Lee S, and Schatz JH (2021) Proteomics reveal cap-dependent translation inhibitors remodel the translation machinery and translome. *Cell Rep* 37:109806.
- Jacklet JW (1977) Neuronal circadian rhythm: phase shifting by a protein synthesis inhibitor. *Science* 198:69-71.

- Jackson RJ, Hellen CU, and Pestova TV (2010) The mechanism of eukaryotic translation initiation and principles of its regulation. *Nat Rev Mol Cell Biol* 11:113-127.
- Jacob H, Curtis AM, and Kearney CJ (2020) Therapeutics on the clock: Circadian medicine in the treatment of chronic inflammatory diseases. *Biochem Pharmacol* 182:114254.
- Janich P, Arpat AB, Castelo-Szekely V, Lopes M, and Gatfield D (2015) Ribosome profiling reveals the rhythmic liver transcriptome and circadian clock regulation by upstream open reading frames. *Genome Res* 25:1848-1859.
- Kantarjian HM, O'Brien S, and Cortes J (2013) Homoharringtonine/omacetaxine mepesuccinate: the long and winding road to food and drug administration approval. *Clin Lymphoma Myeloma Leuk* 13:530-533.
- Kramer A, Lange T, Spies C, Finger AM, Berg D, and Oster H (2022) Foundations of circadian medicine. *PLoS Biol* 20:e3001567.
- Kreutzer FP, Meinecke A, Mitzka S, Hunkler HJ, Hobuss L, Abbas N, Geffers R, Weusthoff J, Xiao K, Jonigk DD, Fiedler J, and Thum T (2022) Development and characterization of anti-fibrotic natural compound similars with improved effectivity. *Basic Res Cardiol* 117:9.
- Leclerc GM, Boockfor FR, Faught WJ, and Frawley LS (2000) Development of a destabilized firefly luciferase enzyme for measurement of gene expression. *Biotechniques* 29:590-591, 594-596, 598 passim.
- Li C, Dong L, Su R, Bi Y, Qing Y, Deng X, Zhou Y, Hu C, Yu M, Huang H, Jiang X, Li X, He X, Zou D, Shen C, Han L, Sun M, Skibbe J, Ferchen K, Qin X, Weng H, Huang H, Song C, Chen J, and Jin J (2020) Homoharringtonine exhibits potent anti-tumor effect and modulates DNA epigenome in acute myeloid leukemia by targeting SP1/TET1/5hmC. *Haematologica* 105:148-160.
- Lu K, Savaraj N, Feun LG, Guo ZG, Umsawasdi T, and Loo TL (1988) Pharmacokinetics of homoharringtonine in dogs. *Cancer Chemother Pharmacol* 21:139-142.
- Luck S, Thurley K, Thaben PF, and Westermarck PO (2014) Rhythmic degradation explains and unifies circadian transcriptome and proteome data. *Cell Rep* 9:741-751.
- Martin-Burgos B, Wang W, William I, Tir S, Mohammad I, Javed R, Smith S, Cui Y, Arzavala J, Mora D, Smith CB, van der Vinne V, Molyneux PC, Miller SC, Weaver DR, Leise TL, and Harrington ME (2022) Methods for Detecting PER2:LUCIFERASE Bioluminescence Rhythms in Freely Moving Mice. *J Biol Rhythms* 37:78-93.
- Montaigne D, Marechal X, Modine T, Coisne A, Mouton S, Fayad G, Ninni S, Klein C, Ortman S, Seunes C, Potelle C, Berthier A, Gheeraert C, Piveteau C, Deprez R, Eeckhoutte J, Duez H, Lacroix D, Deprez B, Jegou B, Koussa M, Edme JL, Lefebvre P, and Staels B (2018) Daytime variation of perioperative myocardial injury in cardiac surgery and its prevention by Rev-Erbalpha antagonism: a single-centre propensity-matched cohort study and a randomised study. *Lancet* 391:59-69.
- Mukherji A, Dachraoui M, and Baumert TF (2020) Perturbation of the circadian clock and pathogenesis of NAFLD. *Metabolism* 111S:154337.
- Mullany LK, Rohira AD, Leach JP, Kim JH, Monroe TO, Ortiz AR, Stork B, Gaber MW, Sarkar P, Sikora AG, Rosengart TK, York B, Song Y, Dacso CC, Lonard DM, Martin JF, and O'Malley BW (2020) A steroid receptor coactivator stimulator (MCB-613) attenuates adverse remodeling after myocardial infarction. *Proc Natl Acad Sci U S A* 117:31353-31364.
- Muller C, Obermann W, Karl N, Wendel HG, Taroncher-Oldenburg G, Pleschka S, Hartmann RK, Grunweller A, and Ziebuhr J (2021) The rocaglate CR-31-B (-) inhibits SARS-CoV-2 replication at non-cytotoxic, low nanomolar concentrations in vitro and ex vivo. *Antiviral Res* 186:105012.
- Nakahara T, Kita A, Yamanaka K, Mori M, Amino N, Takeuchi M, Tominaga F, Hatakeyama S, Kinoyama I, Matsuhisa A, Kudoh M, and Sasamata M (2007) YM155, a novel small-molecule survivin suppressant, induces regression of established human hormone-refractory prostate tumor xenografts. *Cancer Res* 67:8014-8021.
- Olesiak W, Ungar A, Johnson CH, and Hastings JW (1987) Are protein synthesis inhibition and phase shifting of the circadian clock in *Gonyaulax* correlated? *J Biol Rhythms* 2:121-138.

- Ren Y, Wu S, Burdette JE, Cheng X, and Kinghorn AD (2021) Structural Insights into the Interactions of Digoxin and Na(+)/K(+)-ATPase and Other Targets for the Inhibition of Cancer Cell Proliferation. *Molecules* 26.
- Shahid M, and Shahzad-UI-Hussan S (2021) Structural insights of key enzymes into therapeutic intervention against SARS-CoV-2. *J Struct Biol* 213:107690.
- Sinturel F, Gerber A, Mauvoisin D, Wang J, Gatfield D, Stubblefield JJ, Green CB, Gachon F, and Schibler U (2017) Diurnal Oscillations in Liver Mass and Cell Size Accompany Ribosome Assembly Cycles. *Cell* 169:651-663 e614.
- Subramanian A, Narayan R, Corsello SM, Peck DD, Natoli TE, Lu X, Gould J, Davis JF, Tubelli AA, Asiedu JK, Lahr DL, Hirschman JE, Liu Z, Donahue M, Julian B, Khan M, Wadden D, Smith IC, Lam D, Liberzon A, Toder C, Bagul M, Orzechowski M, Enache OM, Piccioni F, Johnson SA, Lyons NJ, Berger AH, Shamji AF, Brooks AN, Vrcic A, Flynn C, Rosains J, Takeda DY, Hu R, Davison D, Lamb J, Ardlie K, Hogstrom L, Greenside P, Gray NS, Clemons PA, Silver S, Wu X, Zhao WN, Read-Button W, Wu X, Haggarty SJ, Ronco LV, Boehm JS, Schreiber SL, Doench JG, Bittker JA, Root DE, Wong B, and Golub TR (2017) A Next Generation Connectivity Map: L1000 Platform and the First 1,000,000 Profiles. *Cell* 171:1437-1452 e1417.
- Sulli G, Manoogian ENC, Taub PR, and Panda S (2018) Training the Circadian Clock, Clocking the Drugs, and Drugging the Clock to Prevent, Manage, and Treat Chronic Diseases. *Trends Pharmacol Sci* 39:812-827.
- Sullivan KA, Grant CV, Jordan KR, Obrietan K, and Pyter LM (2022) Paclitaxel chemotherapy disrupts behavioral and molecular circadian clocks in mice. *Brain Behav Immun* 99:106-118.
- Tamai TK, Nakane Y, Ota W, Kobayashi A, Ishiguro M, Kadofusa N, Ikegami K, Yagita K, Shigeyoshi Y, Sudo M, Nishiwaki-Ohkawa T, Sato A, and Yoshimura T (2018) Identification of circadian clock modulators from existing drugs. *EMBO Mol Med* 10.
- Tan GT, Kinghorn AD, Hughes SH, and Pezzuto JM (1991) Psychotrine and its O-methyl ether are selective inhibitors of human immunodeficiency virus-1 reverse transcriptase. *J Biol Chem* 266:23529-23536.
- Tang R, Jia L, Li Y, Zheng J, and Qi P (2021) Narciclasine attenuates sepsis-induced myocardial injury by modulating autophagy. *Aging (Albany NY)* 13:15151-15163.
- Tujebajeva RM, Graifer DM, Karpova GG, and Ajtkhozina NA (1989) Alkaloid homoharringtonine inhibits polypeptide chain elongation on human ribosomes on the step of peptide bond formation. *FEBS Lett* 257:254-256.
- van der Veen DR, Shao J, Xi Y, Li L, and Duffield GE (2012) Cardiac atrial circadian rhythms in *PERIOD2::LUCIFERASE* and *per1:luc* mice: amplitude and phase responses to glucocorticoid signaling and medium treatment. *PLoS One* 7:e47692.
- Vandel J, Gheeraert C, Staels B, Eeckhoutte J, Lefebvre P, and Dubois-Chevalier J (2020) GIANT: galaxy-based tool for interactive analysis of transcriptomic data. *Sci Rep* 10:19835.
- Vatine G, Vallone D, Appelbaum L, Mracek P, Ben-Moshe Z, Lahiri K, Gothilf Y, and Foulkes NS (2009) Light directs zebrafish *period2* expression via conserved D and E boxes. *PLoS Biol* 7:e1000223.
- Vinod M, Berthier A, Maréchal X, Gheeraert C, Boutry R, Delhaye S, Annicotte J-S, Duez H, Hovasse A, Cianféroni S, Moutaigne D, Eeckhoutte J, Staels B, and Lefebvre P (2022) Timed use of digoxin prevents heart ischemia–reperfusion injury through a REV-ERB α –UPS signaling pathway. *Nature Cardiovascular Research* 1:990-1005.
- Vollmers C, Panda S, and DiTacchio L (2008) A high-throughput assay for siRNA-based circadian screens in human U2OS cells. *PLoS One* 3:e3457.
- Wang C, Lutes LK, Barnoud C, and Scheiermann C (2022) The circadian immune system. *Sci Immunol* 7:eabm2465.
- Wang H, Wang R, Huang D, Li S, Gao B, Kang Z, Tang B, Xie J, Yan F, Liang R, Li H, and Yan J (2021) Homoharringtonine Exerts Anti-tumor Effects in Hepatocellular Carcinoma Through Activation of the Hippo Pathway. *Front Pharmacol* 12:592071.

- Wang L, Yu Y, Chow DC, Yan F, Hsu CC, Stossi F, Mancini MA, Palzkill T, Liao L, Zhou S, Xu J, Lonard DM, and O'Malley BW (2015) Characterization of a Steroid Receptor Coactivator Small Molecule Stimulator that Overstimulates Cancer Cells and Leads to Cell Stress and Death. *Cancer Cell* 28:240-252.
- Wang Z, Lachmann A, Keenan AB, and Ma'Ayan A (2018) L1000FWD: fireworks visualization of drug-induced transcriptomic signatures. *Bioinformatics* 34:2150-2152.
- Watanabe K, Katagai T, Ishida N, and Yamaoka S (1995) Anisomycin induces phase shifts of circadian pacemaker in primary cultures of rat suprachiasmatic nucleus. *Brain Res* 684:179-184.
- Westermarck PO, and Herzog H (2013) Mechanism for 12 hr rhythm generation by the circadian clock. *Cell Rep* 3:1228-1238.
- Yakhni M, Briat A, El Guerrab A, Furtado L, Kwiatkowski F, Miot-Noirault E, Cachin F, Penault-Llorca F, and Radošević-Robin N (2019) Homoharringtonine, an approved anti-leukemia drug, suppresses triple negative breast cancer growth through a rapid reduction of anti-apoptotic protein abundance. *Am J Cancer Res* 9:1043-1060.
- Ye C, Ho DJ, Neri M, Yang C, Kulkarni T, Randhawa R, Henault M, Mostacci N, Farmer P, Renner S, Ihry R, Mansur L, Keller CG, McAllister G, Hild M, Jenkins J, and Kaykas A (2018) DRUG-seq for miniaturized high-throughput transcriptome profiling in drug discovery. *Nat Commun* 9:4307.
- Yoo SH, Yamazaki S, Lowrey PL, Shimomura K, Ko CH, Buhr ED, Slepka SM, Hong HK, Oh WJ, Yoo OJ, Menaker M, and Takahashi JS (2004) PERIOD2::LUCIFERASE real-time reporting of circadian dynamics reveals persistent circadian oscillations in mouse peripheral tissues. *Proc Natl Acad Sci U S A* 101:5339-5346.
- Young SK, and Wek RC (2016) Upstream Open Reading Frames Differentially Regulate Gene-specific Translation in the Integrated Stress Response. *J Biol Chem* 291:16927-16935.
- Zhao X, Hirota T, Han X, Cho H, Chong LW, Lamia K, Liu S, Atkins AR, Banayo E, Liddle C, Yu RT, Yates JR, 3rd, Kay SA, Downes M, and Evans RM (2016) Circadian Amplitude Regulation via FBXW7-Targeted REV-ERB α Degradation. *Cell* 165:1644-1657.
- Zhou Y, Zhou Y, Yang M, Wang K, Liu Y, Zhang M, Yang Y, Jin C, Wang R, and Hu R (2019) Digoxin sensitizes gemcitabine-resistant pancreatic cancer cells to gemcitabine via inhibiting Nrf2 signaling pathway. *Redox Biol* 22:101131.